

# Large optical photon sieve

Geoff Andersen

Laser and Optics Research Center, HQ USAFA/DFP, Suite 2A31, 2354 Fairchild Drive,  
United States Air Force Academy, Colorado 80840

Received June 8, 2005; accepted July 18, 2005

A photon sieve with  $10^7$  holes has been constructed for operation at optical wavelengths. Details of the design, fabrication, and performance of this device are presented. The 1 m focal-length, 0.1 m diameter element is diffraction limited over a significant bandwidth and has a moderate field of view. © 2005 Optical Society of America

OCIS codes: 050.1970, 350.1260, 110.6770, 050.1960.

Diffraction optics offer an appealing solution for the construction of next-generation, ultralarge ( $>20$  m) space telescope primaries.<sup>1–3</sup> A flat element can be simply packaged and deployed without many of the problems associated with creating a diffraction-limited, three-dimensional mirror surface. The diffractive element considered in this case is a photon sieve,<sup>4–8</sup> which is based on a traditional Fresnel zone plate (FZP).<sup>9–12</sup> Unlike a FZP, the photon sieve has no connected regions, thus permitting the fabrication of a single surface without any supporting struts required. Furthermore, apodization is easily incorporated into a photon sieve simply by modifying the number of holes per zone.

A photon sieve is essentially a FZP in which the rings have been broken up into isolated circular holes. For an infinite conjugate, binary FZP of focal length  $f$  at wavelength  $\lambda$ , the radial distance to the center of the  $n$ th bright zone is given by  $r_n$ :

$$r_n^2 = 2nf\lambda + n^2\lambda^2. \quad (1)$$

The width ( $w$ ) of each zone is such that the area is a constant  $\pi\lambda f$ , so

$$w = \frac{\lambda f}{2r_n}. \quad (2)$$

In its simplest version, the photon sieve consists of holes of diameter  $w$  located at a corresponding radial distance  $r_n$ . The holes can be distributed regularly or randomly in angle about the zone. Since the Rayleigh angular resolution of this sieve will be directly proportional to the smallest hole (largest  $r_n$ ), we would typically want  $w$  to be minimized. The constraints on the design then become a combination of the smallest feature that can be printed and the diffractive losses in throughput.

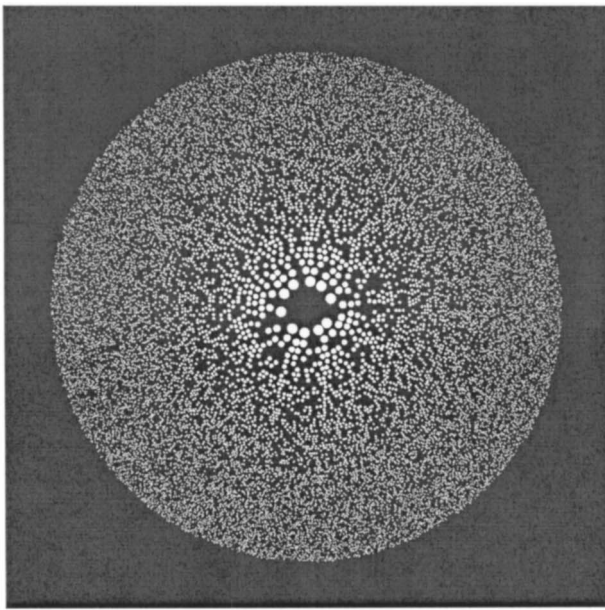
Kipp *et al.*<sup>4</sup> have shown that the size of the holes can be increased beyond the underlying zone width to permit the construction of a large optic with holes of a reasonable size. The effective contribution from an enlarged hole size ( $d$ ) is given by the oscillating function<sup>5</sup>

$$F \propto \frac{d}{w} J_1\left(\frac{\pi d}{2w}\right), \quad (3)$$

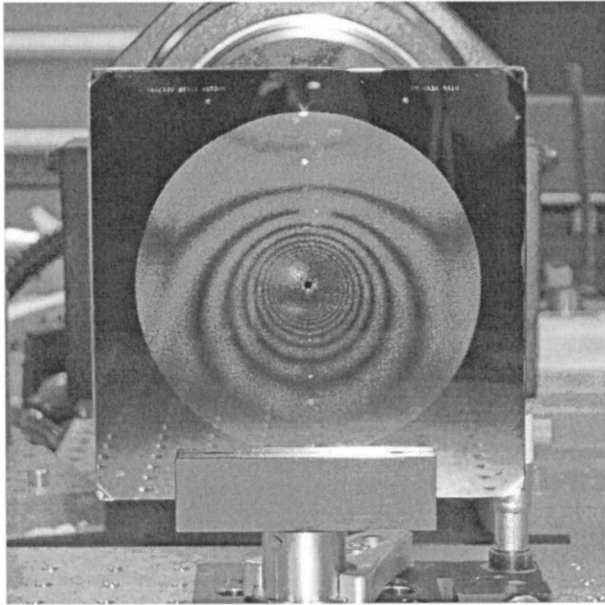
where  $J_1$  is a first-order Bessel function. When  $F > 0$ , light passing through the holes is making a positive contribution to the focused light, and when  $F < 0$  the transmitted light is acting to reduce the focused intensity. More simply, we can understand this in terms of the area of the holes compared to the underlying bright zone.<sup>4–8</sup> Increasing the hole size relative to the underlying bright zone (by a factor  $d/w$ ) will continue to give a positive contribution to the focus so long as the overlap with the underlying bright zone is greater than the overlap with any region of the dark zone.  $F$  increases from zero to a maximum (optimum value) at  $d/w = 1.53$  and then decreases to zero at  $d/w = 2.44$ . The oscillating nature of the function is such that larger ratios of  $d/w$  are possible but are the result of less-efficient, higher-order diffraction and thus are ignored here. The increase in hole diameters provided by this theory greatly reduces the design constraints on fabricating such a device.

A photon sieve was designed with a focal length of 1.0 m and a diameter of 0.1 m to operate at a wavelength of 532 nm. The angular positions of 10,035,344 holes on 2349 rings ( $n = 2–2350$ ) were generated randomly and such that they did not overlap. The resolution of the fabrication process was  $0.1 \mu\text{m}$ , so it was decided that a minimum acceptable diameter for the holes would be set at  $10 \mu\text{m}$  to give the best registration and hole sharpness. This limitation meant that the hole diameters were set at 1.53 times the underlying zone width until the zones became smaller than  $6.54 \mu\text{m}$  (at roughly 80% of the way to the edge). From that point outward the hole diameters were kept at a constant  $10 \mu\text{m}$  to the edge of the photon sieve. Since the outer zone has a width of  $5.32 \mu\text{m}$ , the maximum  $d/w$  factor is 1.88, which is still comfortably below the limit of 2.44. Figure 1(a) shows an image of the central 20 mm diameter of the photon sieve, with rings of order  $n = 2–100$ . The largest holes ( $n = 2$ , in the center ring) are  $279 \mu\text{m}$  in diameter.

The size and positional data for the holes were converted into an image file format, which was then used as a basis for the fabrication. Electron-beam lithographic process was used to produce the photon sieve



(a)



(b)

Fig. 1. (a) Central 99 rings (20 mm diameter) of the  $10^7$  hole photon sieve. (b) Actual photon sieve illuminated from the rear. The regular underlying ring pattern results in the appearance of moiré fringes across the plate.

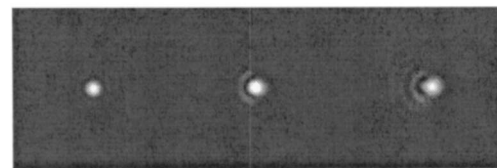
on a chrome-coated, 125 mm square, 2.4 mm thick quartz plate. A frequency-doubled Nd:YAG laser ( $\lambda = 532$  nm) was spatially filtered and directed onto a high-quality achromat lens to create a diffraction-limited collimated beam. An image of the photon sieve as lit by this beam is shown in Fig. 1(b). As expected, the photon sieve focused the collimated light onto a focal spot 1 m away. The ratio of the total power in the focal spot to that incident upon the photon sieve was 0.35%. The performance of the photon sieve was then evaluated in several ways, by focusing, imaging, and interferometry.

The diameter of the central maximum of the focal spot was  $13.7 \pm 0.5 \mu\text{m}$ , compared to the expected diffraction-limited spot size of  $13.0 \mu\text{m}$ . Images were then obtained at regular intervals on either side of the focus [Fig. 2(a)]. The symmetry of their appearance (in a so-called star test) indicates a negligible amount of spherical aberration or astigmatism. Next, the photon sieve was tilted to assess the off-axis focusing performance. Figure 2(b) shows the focal spots for  $0^\circ$ ,  $0.25^\circ$ , and  $0.5^\circ$  off-axis angles. Modeling with optical design software shows that the diffraction-limited field of view is expected to be  $0.5^\circ$ .

The focused light from the photon sieve was recollimated with a high-quality achromat and made to interfere with a diffraction-limited reference beam. Figure 3(a) shows the interferogram imaged back to the surface of the photon sieve ( $\lambda = 532$  nm). An analysis of the interferogram gave a wavefront error of  $0.21\lambda$  peak to valley,  $0.04\lambda$  rms, and a Strehl ratio of 0.94. A second interferogram was made, this time with light from a green helium–neon laser at a wavelength of 543.4 nm [Fig. 3(b)]. The resultant wavefront aberration was calculated to be  $0.25\lambda$  peak to valley and  $0.05\lambda$  rms and to have a Strehl ratio of 0.9. These values are significant, as they indicate a diffraction-limited operation over a useful bandwidth. It should also be noted that the actual performance of the photon sieve will be much better than these interferograms suggest, as they include the wavefront errors of three lenses, one mirror, and a beam splitter.

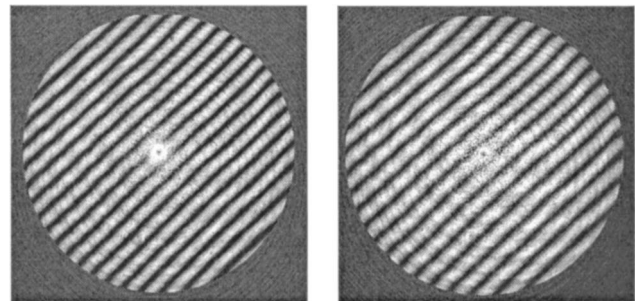


(a)



(b)

Fig. 2. Focal spots: (a) images of the focused beam at regular locations on either side of the focus, (b) images of the focal spot at, left to right,  $0^\circ$ ,  $0.25^\circ$ , and  $0.5^\circ$  off axis.



(a)

(b)

Fig. 3. Interferogram of the photon sieve, showing diffraction-limited performance at (a) the design wavelength of 532 nm and (b) the green helium–neon wavelength of 543.4 nm.

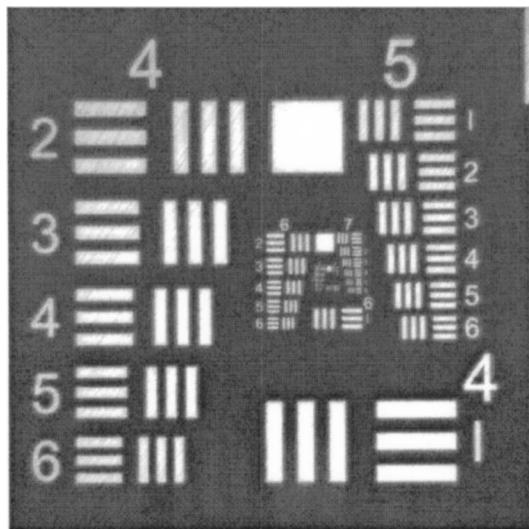


Fig. 4. Resolution test target imaged with the photon sieve at 532 nm.

The spatial filter used for illuminating the collimator was replaced with a 1951 U.S. Air Force resolution test target illuminated by laser light passed through a rotating diffuser to remove speckle. The image of the target produced by the photon sieve at 532 nm is shown in Fig. 4. In this image, group 7, element 2 is resolved as would be expected from a diffraction-limited lens of diameter 0.1 m and focal length 1 m. In fact, images taken by using both green and red helium–neon wavelengths (543.4 and 632.9 nm, respectively) also demonstrated that diffraction-limited imaging is possible over a large bandwidth.

In conclusion, these experiments demonstrate the feasibility of using a photon sieve as the primary el-

ement in an optical telescope. A 0.1 m diameter, 1 m focal-length photon sieve was fabricated with  $10^7$  holes ranging in size from 10 to 279  $\mu\text{m}$ . The performance of the photon sieve was evaluated in several ways, indicating diffraction-limited focusing. Future experiments will be aimed at developing methods for reducing the dispersive effects for broadband imaging as well as toward fabricating a membrane version suitable for deployment in space.

The author acknowledges the support of this research by the U.S. Air Force Office of Scientific Research. G. Andersen's e-mail address is geoff.andersen@usafa.af.mil.

#### References

1. M. Barton, J. A. Britten, S. N. Dixit, L. J. Summers, I. M. Thomas, M. C. Rushford, K. Lu, R. A. Hyde, and M. D. Perry, *Appl. Opt.* **40**, 447 (2001).
2. A. B. Meinel and M. P. Meinel, *Appl. Opt.* **41**, 7155 (2002).
3. A. B. Meinel and M. P. Meinel, *Opt. Eng.* **41**, 1995 (2002).
4. L. Kipp, M. Skibowski, R. L. Johnson, R. Berndt, R. Adelung, S. Harm, and R. Seemann, *Nature* **414**, 184 (2001).
5. Q. Cao and J. Jahns, *J. Opt. Soc. Am. A* **19**, 2387 (2002).
6. Q. Cao and J. Jahns, *J. Opt. Soc. Am. A* **20**, 1005 (2003).
7. Q. Cao and J. Jahns, *J. Opt. Soc. Am. A* **20**, 1576 (2003).
8. Q. Cao and J. Jahns, *J. Opt. Soc. Am. A* **21**, 561 (2004).
9. G. S. Waldman, *J. Opt. Soc. Am.* **56**, 215 (1966).
10. H. H. M. Chau, *Appl. Opt.* **8**, 1209 (1969).
11. V. E. Levashov and A. V. Vinogradov, *Phys. Rev. E* **49**, 5797 (1994).
12. C. M. Choy and L. M. Cheng, *Appl. Opt.* **33**, 794 (1994).